Multifocal Ectopic Purkinje-related Premature Contractions: a new *SCN5A*-related cardiac channelopathy

Gabriel Laurent, MD, PhD,* Samuel Saal, MD,† Mohamed Yassine Amarouch, PhD,‡§‖ Delphine M Béziau, MSc,‡§‖ Roos FJ Marsman, MSc,¶ Laurence Faivre, MD, PhD,† Julien Barc, PhD,‡‖ Christian Dina, PhD,‡‖ Geraldine Bertaux, MD,* Olivier Barthez, MD,* Christel Thauvin-Robinet, MD,PhD† Philippe Charron, MD, PhD,# Véronique Fressart, MD, PhD,** Alice Maltret, MD, †† Elisabeth Villain, MD, †† Estelle Baron, BA,‡‖ Jean Mérot, PhD,‡§‖ Rodolphe Turpault, PhD, ‡‡‖ Yves Coudière, PhD, ‡‡‖ Flavien Charpentier, PhD,‡§‖§§ Jean Jacques Schott, PhD,‡‖§§ Gildas Loussouarn, PhD,‡§‖ Arthur A. M. Wilde, MD, PhD,¶ Jean Eric Wolf, MD, PhD,* Isabelle Baró, PhD,‡§‖ Florence Kyndt, PharmD, PhD,‡‖ ‖‖ Vincent Probst, MD, PhD.‡‖§§

Drs Laurent, Saal, and Amarouch contributed equally to this work.

Drs Baró, Kyndt and Pr Probst contributed equally to this work as senior authors.

Address correspondence to: Gabriel LAURENT, MD-PhD, Service de Cardiologie, 2 Boulevard Maréchal De Lattre de Tassigny, 21079 Dijon Cedex, France, Phone: +33 3.80.29.33.13; Fax : +33 3.80.29.33.33; e-mail: gabriel.laurent@chu-dijon.fr

Brief title: Laurent *et al.* - MEPPC: a new *SCN5A*-related cardiac channelopathy

***J. Am. Coll. Cardiol.* 2012; 60:144-156.**

http://dx.doi.org/10.1016/j.jacc.2012.02.052

From * CHU Dijon, Service de Cardiologie, Hôpital le Bocage, Dijon, France; †CHU Dijon, Centre de Génétique, Hôpital d'Enfants, Dijon, France; ‡INSERM, UMR1087, l'institut du thorax, Nantes, France; §CNRS, UMR6291, Nantes, France; ‖Université de Nantes, Nantes, France; ¶Department of Experimental Cardiology, Heart Failure Research Center, Academic Medical Center, Amsterdam, The Netherlands; #AP-HP, GH Pitié Salpêtrière, Département de Cardiologie, and UPMC Univ Paris 6, Département de Génétique, INSERM UMR-S956, Paris, France; **AP-HP, GH Pitié Salpêtrière, UF Cardiogénétique et Myogénétique Moléculaire et Cellulaire, Service de Biochimie Métabolique et Centre de Génétique, Paris, France; ††Cardiologie Pédiatrique, Université Paris V René Descartes, Hôpital Necker-Enfants Malades, Paris, France; ‡‡ CNRS, UMR6629, Laboratoire de Mathématiques Jean Leray, Nantes, France, §§CHU Nantes, l'institut du thorax, France, ‖‖CHU Nantes, Service de génétique médicale, Nantes, France.

Mohamed Yassine Amarouch present address: University of Bern, Department of Clinical Research, Bern Switzerland; Julien Barc, present address: University of Amsterdam, Department of Experimental Cardiology, Academic Medical Center, Amsterdam The Netherlands

Funding sources: The *Agence Nationale de la Recherche* financially supported R.T. and Y.C. (ANR-07-JCJC-0141), I.B. (ANR-09-GENO-003-01) and J.-J.S. (ANR-05-MRAR-028-01). J.-J.S. was also supported by a Leducq Foundation Trans-Atlantic Network of Excellence grant (05 CVD 01). The research leading to these results has also received funding from the *European Community's Seventh Framework Programme* FP7/ 2007-2013 under grant agreement n° FP7-HEALTH-2009-single-stage 241526 (I.B. and F.C.). G.Lo. was financially supported by the *Association*

Française contre les Myopathies (n°14120) and F.C. by the *Fondation pour la Recherche Médicale* (DVC20070409253).

Disclosures: None

ABSTRACT

Objectives - The aim of this study was to describe a new familial cardiac phenotype and to elucidate the electrophysiological mechanism responsible for the disease.

Background - Mutations in several genes encoding ion channels, especially *SCN5A*, have emerged as the basis for a variety of inherited cardiac arrhythmias.

Methods and Results - We identified three unrelated families comprising 21 individuals affected by Multifocal Ectopic Purkinje-related Premature Contractions (MEPPC) characterized by narrow junctional and rare sinus beats competing with numerous premature ventricular contractions with right and/or left bundle branch block patterns. Dilated cardiomyopathy was identified in 6 patients, atrial arrhythmias were detected in 9 patients and sudden death was reported in 5 individuals. Invasive electrophysiological studies demonstrated that premature ventricular complexes originated from the Purkinje tissue. Hydroquinidine treatment dramatically decreased the number of premature ventricular complexes. It normalized the contractile function in two patients. All the affected subjects carried the c.665G>A transition in the *SCN5A* gene. Patch-clamp studies of resulting p.Arg222Gln (R222Q) Nav1.5 revealed a net gain of function of the sodium channel, leading, *in silico,* to incomplete repolarization in Purkinje cells responsible for premature ventricular action potentials. *In vitro* and *in silico* studies recapitulated the normalization of the ventricular action potentials in the presence of quinidine.

Conclusions - We identified a new *SCN5A*-related cardiac syndrome, Multifocal Ectopic Purkinje-related Premature Contractions (MEPPC). The *SCN5A* mutation leads to a gain of function of the sodium channel responsible for hyperexcitability of the fascicular-Purkinje system. The MEPPC syndrome is responsive to hydroquinidine.

Abbreviations list

AF: atrial fibrillation

AP: action potential

CRTD: cardiac resynchronization therapy defibrillator

DCM: dilated cardiomyopathy

DDD PM: DDD pace maker

ICD: implantable cardioverter defibrillator

LBBB: left bundle branch block

LQT: long QT syndrome

LVDd: left ventricular diastolic diameter

LVEF: left ventricular ejection fraction

MEPPC: Multifocal ectopic Purkinje-related premature contractions

PACs: premature atrial complexes

PVCs: premature ventricular complexes

RBBB: right bundle branch block

SD: sudden death

TTE: trans-thoracic echocardiogram

VPB: ventricular premature beat

Primary arrhythmogenic disorders of the heart are a major cause of sudden cardiac death in otherwise healthy individuals with structurally normal hearts. Mutations in several genes encoding ion channels and channel-interacting proteins have emerged over the last decade as the basis for a variety of inherited cardiac arrhythmias (1,2,3). Different mutations in a single gene may account for various disorders depending on the position of the mutation, the nature of the amino acid substituted, the type of the mutation (non sense, false sense…) and its functional consequences (4,5).

The SCN5A gene encodes the pore-forming subunit of the voltage-gated Na^+ channel Nav1.5. In the heart, this channel plays a key role in rapid impulse propagation through the conduction system and in the excitability of atrial and ventricular cardiomyocytes. Mutations in *SCN5A* are responsible for a spectrum of hereditary arrhythmias, including type-3 LQT (LQT3) syndrome, the Brugada syndrome, cardiac conduction disease, sinus node dysfunction, atrial fibrillation and dilated cardiomyopathy (see 6 for a review; 7-9,5,10-13). In addition to these syndromes, originally regarded as independent entities, recent evidence shows considerable clinical overlap, implying new disease entities known as overlap syndromes of the cardiac Na^+ channel (14).

In this article, we report a novel autosomal dominant form of cardiac arrhythmia identified in three unrelated families and characterized by Multifocal Ectopic Purkinje-related Premature Contractions (MEPPC). This arrhythmia is due to the c.665G>A *SCN5A* mutation leading to a shift in p.Arg222Gln (R222Q) Nav1.5 voltage-dependency.

METHODS

An expanded Methods section is available in an online data supplement.

Clinical evaluation

This study was in agreement with the local guidelines for genetic research and has been approved by the local ethical committees. Informed, written consent was obtained from each family member who agreed to participate to the study. Standard 12-lead ECG, Holter recording and echocardiography were proposed to all participating family members. We also proposed electrophysiological studies (EP) to some patients.

Patients were considered affected when ventricular arrhythmia corresponding to multifocal ectopic Purkinje-related premature contractions was detected.

Mutation analysis

Genomic DNA was extracted from peripheral blood lymphocytes using standard protocols. The proband (III.1) of family 1 was screened for mutations in known genes responsible for DCM and arrhythmia, including *LMNA* encoding lamin A/*C*, *ABCC9* encoding SUR2A and *SCN5A* (15,16,10).

Haplotype Analysis

Ten microsatellite markers around the *SCN5A* gene (D3S1759, D3S2432, D3S3047, D3S3512, D3S1298, intragenic *SCN5A* marker, D3S3521, D3S3527, D3S3522 and D3S3559) were genotyped. We estimated the age of the mutation using the Genin and collaborators' method (17).

Cellular electrophysiology

Patch-clamp studies were performed on COS-7 cells transiently expressing human WT or R222Q Nav1.5 (NG_008934) and human ß1 subunits, using the whole-cell configuration at room temperature (18).

Mathematical modeling

Single-cell models of the human Purkinje cells (19) and left-ventricular myocytes (20) were used. Both models were incorporated in a multicellular model and the propagation of the electrical waves in the cardiac tissues was described by a monodomain model (21). The numerical simulations were performed on a simplified 2D slice model described previously (22).

Statistics

All data are presented as mean ± SEM. The statistical significance of the observed effects was assessed by the Student *t*-test or 2-way ANOVA followed by a Tukey test for multiple comparisons when needed. A value of $p<0.05$ was considered significant.

RESULTS

We identified 3 families affected by the same phenotype, segregating with an autosomal dominant pattern over three generations (Figure 1A). In Family 1, 11 individuals out of 18 family members were affected , 4 individuals out of 5 in Family 2 and 6 individuals out of 8 in Family 3. Patient characteristics are summarized in Tables 1 and 2.

Clinical results

Clinical phenotype of the Family 1 proband (patient III.1)

Patient III.1 was identified at the age of 10 after mild dyspnea while exercising. Her 12-lead surface ECG showed a chaotic cardiac rhythm comprising narrow junctional and rare sinus beats competing with premature ventricular complexes (PVCs) showing various right bundle branch block (RBBB) patterns (Figure 2A). There was an overdrive suppression of the PVCs during treadmill exercising. Signal averaged

ECG did not show late potentials. A Holter monitoring device recorded more than 50000 PVCs per 24 h. The trans-thoracic echocardiogram (TTE) revealed a mild dilation of the left ventricle (left ventricular diastolic diameter, LVDd: 54 mm or 40 mm/m^2, above 97^{th} percentile) (23), but a normal left ventricular ejection fraction (LVEF: 62%). She remained asymptomatic until the age of 13 when she was referred for brief sudden loss of consciousness at rest. The ECG exhibited recurrent non-sustained ventricular tachyarrhythmias (NSVTs) with RBBB patterns, which were concomitant with several fainting episodes (Figure 2B). Several non sustained supra-ventricular arrhythmias have been identified during the follow-up. New TTE showed a markedly enlarged LVDd (62 mm), and a decreased LVEF (32%). A dual-chamber implantable cardioverter-defibrillator (ICD) was then implanted associated with oral hydroquinidine treatment. Once the measured plasma level of the drug reached 1 mg/L (normal range 1-3 mg/L), this medication succeeded in markedly reducing the number of PVCs (Table 2). After one year under hydroquinidine treatment, the PVC burden was <1% and her heart was considered normal in TTE (LVDd: 54 mm, LVEF: 56%).

Clinical investigation of family members allowed the identification of 10 other affected individuals with similar ECG characteristics (Supplemental Figure 1).

Clinical phenotype of the Family 2 proband (patient III.1) and his twin brother (patient III.2)

Patient III.1 was identified at age 6 because of an irregular heart rate without any other symptoms. His twin brother was diagnosed at 12 years with the same arrhythmia after experiencing syncope while cycling. A complete clinical evaluation including a TTE and a MRI was normal, but his ECG showed frequent PVCs with a

left bundle branch block (LBBB) pattern, and superior and inferior axial deviation (Figure 2C). In both patients, the Holter ECG recorded tens of thousands of PVCs per 24 hours (Table 1). Exercise allowed a clear decrease of their number. Both patients were finally treated with hydroquinidine, leading to a dramatic decrease of the PVC number (Table 2).

Their father and grandmother had both been affected with DCM associated with frequent PVCs, and one uncle, known as affected by atrial flutter, had died suddenly at age 11.

Clinical phenotype of the Family 3 proband (patient II.3)

The index patient II-3 was identified at the age of 18 during a routine medical examination. Her 12-lead ECG showed premature atrial complexes (PACs), atrial fibrillation (AF), pre-excitation on the ECG, and frequent relatively narrow PVCs with both LBBB and RBBB patterns. Electrophysiological testing revealed ectopic foci from the atria, the AV junction and the bundle branches. The accessory pathway was located at the right septal site. At the age of 48, Holter monitoring recorded a permanent chaotic supraventricular rhythm with >48900 PACs and >7000 isolated and bigeminal PVCs (35% and 5% of total QRS complexes, respectively). Flecainide therapy marginally reduced ventricular ectopies however completely suppressed supraventricular arrhythmia (Holter monitoring recorded <150 PACs, representing <1% of total QRS complexes). Flecainide therapy was maintained since hydroquinidine is not available in the Netherlands, where Family 3 lives.

A remarkably constant phenotype

Within these 3 families, 21 individuals were affected by PVCs. Patient characteristics are summarized in Tables 1 and 2. Despite the various ages at diagnosis, from 24

weeks of gestation to 62 years (mean age: 20 years; n = 20), the phenotype was remarkably constant: narrow sinus and junctional QRS complexes (17 individuals) competing with various complexes showing a RBBB or LBBB patterns (15 individuals), corresponding to PVCs with superior or inferior axes. We did not observe any QT prolongation (Table 1) or ST segment elevation.

PVCs were isolated, or paired (bigeminism) with sinus or junctional QRS complexes. NSVTs were identified in 8 individuals. Five patients were affected by syncope or presyncope. Sudden death was reported in one 4-month-old boy (III.12 in family 1), an 11-year-old boy (II.3 in family 2) and three adult males (29, 50 and 71 years old; II.7 and I.1 in family 1 and I.1 in family 3). However, PVCs were clearly identified in only two of these cases (II.7 in family 1 and I.1 in family 3) before sudden death. Episodes of syncope or fainting during polymorphic VT episodes (Holter or ICD monitorings) were reported in 3 females (figure 2B). Two individuals in family 1, 1 in family 2, and 6 in family 3 presented with atrial arrhythmia (PACs, non sustained atrial tachy-arrhythmia or AF). One patient had AV conduction disturbances. Only one patient in family 3 had an accessory pathway.

Electrophysiological study

EP testing was performed in 7 cases (Figure 3 and Supplemental Figure 2). Presystolic potentials recorded at ectopic sites during PVCs either corresponded to Purkinje potentials during normal sinus beats or to the proximal extension of the left anterior and posterior fascicles (Figure 3B-C). In all tested patients, numerous ectopic foci were identified along the left conduction system and its proximal extension. We did not record any PVCs from the myocardium itself as the local ventricular electrograms were always preceded by a Purkinje potential and we did not

record any retrograde Purkinje potential activation or slow conduction area in the Purkinje network. Reentrant mechanisms were excluded since no PVCs or VTs could be pacing induced and no mid-diastolic potentials were recorded during VT (24-26). When tried on patient II.4 of family 1, radiofrequency applications did not eradicate PVCs as the whole Purkinje tissue was involved in triggering PVCs from varying sites. Whereas we proposed EP studies to most of the patients, not all of them accepted. Among affected members in the three families, PVC features were very similar with a sharp slope of the first ventricular deflection and close characteristics to authentic LBBB or RBBB patterns with right or left axis. In patients who underwent an EP study, we identified those PVC morphologies as being triggered from Purkinje fibers. We therefore inferred that similar PVC patterns may originate from similar Purkinje regions in the other patients.

Evolution of the left ventricular function on anti-arrhythmic treatment.

TTEs were performed in all affected patients and an MRI in 3 cases. Low LVEF with dilation of the left ventricle was identified in 7 patients. Several anti-arrhythmic treatments were attempted within the families (Table 2). Amiodarone treatment was partially successful in 2 cases (patient II.6 family 1 and patient II.1 family 2). For patient II.1 family 2, amiodarone and CRTD treatment were introduced simultaneously, partially normalizing the LVEF (from 20% to 45%). Hydroquinidine was successful in 5 cases with a dramatic decrease in the number of PVCs per 24 hours (Table 2), and dramatically decreased the PVCs number and improved the ventricular function in all cases. Patient III.1 was the first person to be treated by Hydroquinidine in family 1 and no adverse effects were noticed after four years of follow-up. Flecainide therapy was used in 5 patients and greatly reduced

supraventricular and ventricular arrhythmias, with a clear decline in ventricular tachycardia episodes, in 3 of them. Other anti-arrhythmic drugs were used in 4 patients but were successful in 3 cases only (Table 2).

ICD was implanted in 4 patients, two of which had a cardiac resynchronization therapy defibrillator. Only one patient (family 3) had atrioventricular conduction disturbances and was implanted with a double chamber pacemaker (Table 2).

Genetic results

Mutation analysis

Since the first proband identified (family 1, III.1) had DCM, mutations in *LMNA* encoding lamin A/*C* and *ABCC9* encoding SUR2A, genes reported to be associated with DCM, were searched in this patient although unsuccessfully. *SCN5A* gene, reported to be associated with DCM and various arrhythmogenic diseases, was also sequenced. Genetic testing of family 1's proband revealed that she was heterozygous for a c.665G>A transition in *SCN5A* exon 6 (Figure 1B), resulting in the substitution of an arginine for a glutamine at position 222 (p.Arg222Gln named R222Q, subsequently). This substitution is located in the voltage-sensing S4 segment of domain I of the cardiac Na^+ channel Nav1.5 (Figure 1D). Subsequently, the mutation was detected in family 2's (III.1) and family 3's (II.3) probands who did not present DCM. The mutation was 100% penetrant and strictly segregated with the cardiac arrhythmia in all the families, consistent with a mutation-related disease (Figure 1A). It was absent in 600 control chromosomes. The Arg222 (R222) amino-acid is highly conserved across species (Figure 1C). This mutation is reported on dbSNP (rs45546039) but at 0% in all populations and is not reported in NHLBI Exome variant server.

Haplotype analysis

To investigate whether a common ancestral chromosome accounted for the recurrence of the R222Q mutation in unrelated families 1, 2 and 3, we constructed mutation-associated haplotypes by genotyping family members for ten microsatellite markers (Supplemental Figure 3 and Supplemental Results).

Our data demonstrates that a founder effect for the R222Q mutation in these three families is very unlikely.

Effects of R222Q mutation on Nav1.5 channel function in COS-7 cells

To investigate the functional consequences of the R222Q mutation on the Na^+ channel activity, we used the whole-cell configuration of the patch-clamp technique (see online data supplement). The presence of the mutation did not modify the Na^+ current density (Figure 4A-B and Supplemental Table 1). The activation curve was shifted toward more negative potentials in the presence of the mutation (Figure 4A and Supplemental Table 1). Activation kinetics were accelerated in the mutant (Supplemental Figure 4A; two-way ANOVA, $p<0.001$ *versus* WT). Inactivation voltage sensitivity was also changed (Figure 4B and Supplemental Table 1) which, combined with the activation curve shift, predicted an increase of the window current availability (Supplemental Figure 5A). The maximum conductance of the TTX-sensitive window current elicited by depolarizing-voltage ramps was not significantly different in R222Q Nav1.5 expressing cells but the voltage at which the maximum conductance was measured, was significantly shifted toward more negative values and the window current availability was increased when expressed as the area under I/V curve (t-test $p<0.001$ and $p<0.01$, respectively; Supplemental Table 1 and Figure 4C). Each of these changes caused a gain of function of the mutant channel. However,

inactivation onset kinetics were also accelerated causing a loss of function (Supplemental Figure 4B; two-way ANOVA $p<0.001$ *versus* WT). Finally, kinetics of recovery from inactivation were not significantly modified by the R222Q mutation (Supplemental Figure 4C).

In order to understand the effects of hydroquinidine treatment on PVCs occurrence, we evaluated the WT and R222Q Na^+ current sensitivity to quinidine, its active form. At a concentration at which the WT peak I_{Na} was about half-reduced (30 µM in our conditions; Supplemental Table 2, Figure 4D), WT and R222Q peak currents were similarly inhibited (two-way ANOVA $p<0.001$ *versus* control). When quinidine was tested on the window current, the inhibition was also similar in both groups when measured at the maximum conductance potential of each group (Figure 4D and Supplemental Table 2; two-way ANOVA $p<0.001$ *versus* control). Therefore, WT and R222Q Na^+ currents were equally sensitive to quinidine.

A multicellular computer model to characterize the molecular and cellular events leading to premature ventricular contractions.

Because of the multiple and opposite effects of the mutation on channel activation and inactivation, its net effect on the action potential (AP) is not straightforward. To get insights on this effect, we carried out computer simulations and evaluated the impact of the mutation on AP in single-cell models of human Purkinje fibers and ventricles (see Supplemental Methods and Supplemental Results). Single-cell models of Purkinje and ventricular cell AP were run in WT and heterozygous conditions. In heterozygous conditions, incomplete repolarization occurred in Purkinje cell AP, correlated with an increased late Na^+ current (Supplemental Figure 6). The ventricular AP was much less affected (Supplemental Figure 6).

To evaluate the possibility of a causal role of the mutation on the generation of PVCs, we built a multicellular model incorporating both human cell models. In WT condition, 1-Hz stimulation of the Purkinje fibers generated AP that propagated to the ventricle (Figure 5Ba, Supplemental Movie Aa). Interestingly, in the heterozygous condition, incomplete repolarization in the Purkinje fibers triggered premature APs, propagating into the ventricles (Figure 5Bb, Supplemental Movie Ab). Consistent with the disappearance of clinically observed PVCs during exercise, the triggered ventricular APs disappeared at higher pacing frequencies (2 Hz, Figure 5Cb, Supplemental Movie Bb). Altogether, these results (i) strongly suggest that the gain of function of the Na^+ current predominantly affects the Purkinje cells, (ii) explain the fact that the entire Purkinje system was affected resulting in a wide variety of ectopic foci, and (iii) explain the frequency dependency of the PVCs.

Finally, the effects of quinidine were tested on the multicellular model. Clinically relevant effects of this drug are thought to be due to alteration of the Na^+ current, the transient outward current I_{to} (27,28), and the repolarizing delayed rectifier current I_{Kr} (29,30). In addition, quinidine also inhibits Ca^{2+} and other K^+ currents, although in a lower extent (31,32). Therefore, inhibition of these latter currents was not considered. In the model, the K^+ currents were reduced in parallel with the heterozygous Na^+ current. For the first test, we chose 10 µM quinidine, the maximal therapeutic dose *i.e.* preserving 50% I_{Na}, 30% I_{Kr} (33) and 30% I_{to} (28). In this case, we observed a normalization of the Purkinje and ventricular AP course at 1 Hz (not shown). To evaluate the effects of a more 'therapeutic' dose of quinidine, we ran the model with lower current inhibition levels. As illustrated for the ventricular AP in Figure 5B, the normalization was still observed when the computed quinidine dose was reduced to preserve 75% I_{Na} and 45% I_{Kr} and I_{to}. However, when the computed quinidine dose

was further reduced to preserve 85% I_{Na} and 50% I_{Kr} and I_{to}, triggered APs reappeared. Qualitatively, if not quantitatively, the multicellular model mimics the cardiac response to hydroquinidine treatment.

DISCUSSION

We report a novel autosomal dominant form of cardiac arrhythmia showing multifocal ectopic Purkinje-related premature contractions (MEPPC). MEPPC syndrome is characterized by frequent PVCs originating from various ectopic foci along the fascicular-Purkinje system occasionally associated with non-sustained VTs and sudden death. Some patients (n=9) also presented with PACs, non sustained atrial tachy-arrhythmias or paroxysmal AF. In some patients, arrhythmias were associated with mild DCM. Hydroquinidine markedly reduced the number of PVCs and normalized the left ventricular function in patients with DCM. We demonstrate that a fully penetrant *SCN5A* gain-of-function mutation is responsible for this new syndrome.

Specificity of MEPPC

Ventricular arrhythmias originating from left ventricular fascicles have been described previously in patients with or without structural heart disease (ischemic or idiopathic cardiomyopathies) (34,24,25,35). Accounting for up to 30-50% of arrhythmias in non-ischemic DCM, bundle branch re-entrant VTs usually have a LBBB pattern and enlarged QRS complexes with a prolonged H to V interval during sinus rhythm (34). Such conduction abnormalities were not identified in any of our patients.
Fascicular VT is the most common form of idiopathic left VT occurring more frequently in young males without structural heart disease and with a particular sensitivity to verapamil (24). The ECG characteristics of our patients were different. MEPPC syndrome was distinguished from PVCs originating from the posterior

papillary muscle in the left ventricle (36) mainly by the presence of high-frequency potentials preceding local myocardial activation suggesting that Purkinje system was involved. Idiopathic VTs and bundle branch VTs typically present a single ECG morphology originating either near the posterior or the anterior left fascicle. In our patients, ECG characteristics demonstrated the varying origins of the PVCs, in either the left or right ventricle. EP testing using a 3D endocardial navigation system clearly demonstrated that the PVCs originated from more than 10 different foci along the extension of the left anterior and posterior fascicles. This phenomenon was responsible for important changes in PVCs morphology (shape and axis) from one beat to another. Like triggered activities, the firing was fairly increased by isoproterenol infusion despite the increase in sinus rhythm at a lesser extent. As opposed to idiopathic fascicular VTs which are well known to be highly sensitive to verapamil, this treatment had no effect on the tested affected family members. Atrial arrhythmias were less frequently observed than PVCs.

R222Q mutation causes the syndrome in three unrelated families

Several findings support the causative role of the R222Q *SCN5A* mutation in the pathogenesis of the disease in the three reported families: (i) the complete co-segregation of the mutation with the disease phenotype, (ii) the identification of the same mutation in three unrelated families with a remarkably uniform phenotype, (iii) the absence of the mutation in 300 ethnically matched control individuals and (iv) the high conservation of the R222 residue across species (figure 1C).

R222Q has been reported in a single patient with a Brugada syndrome (37). With the help of Dr Xavier Waintraub (Hôpital Pitié-Salpêtrière, Paris, France) and the kind permission of Dr Pascale Guicheney (INSERM UMR S956, Paris, France), we had

the opportunity to reevaluate the phenotype of this patient. He was clearly not affected by the Brugada syndrome, his ECG presenting no ST segment elevation in the precordial leads. His phenotype appeared to be very closed to that of MEPPC syndrome with permanent junctional activity, very frequent multifocal ventricular premature beats (57000 thin VPBs per day coming from left anterior and posterior fascicles), atrial arrhythmias and dilated cardiomyopathy with moderated alteration of the ventricular contraction (LVEF 56%) (personal communication). His familial history found that his mother and grandmother were also affected by dilated cardiomyopathy associated with frequent PVCs. None of the ECGs performed in patients harboring the *SCN5A* R222Q mutation met the ST segment criteria for a Brugada syndrome. The same *SCN5A* mutation was also detected in a cohort of 2,500 unrelated cases referred for LQTS genetic testing (38). However, none of the patients from the three families here presented a prolonged QTc. This may be explained by the relatively less impaired biophysical properties of the R222Q channel, mostly a negative shift of the window current, when compared to that of already reported LQT3-related mutants (39,5).

R222Q effects that we report on channel parameters were similar to those measured by Cheng et al. (40). In addition, we show that these effects are intermediate in the heterozygous state and that they also impair the window current, crucial during the AP plateau phase.

Looking for a mechanistic link between the genotype and the phenotype, we simulated the effect of the mutated channel activity on the Purkinje and ventricular electrical activity. Two points suggest that the shift in Nav1.5 voltage-dependency is responsible for the premature ventricular contractions originating from the fascicular-Purkinje system. First of all, one of the particularities of this arrhythmia is that ectopic

foci were observed in erratic locations of the Purkinje system, which made radiofrequency applications ineffective. The multicellular model shows that the impaired function of the Na^+ channels, anywhere in the Purkinje system, is sufficient enough to trigger premature APs in the surrounding ventricular tissue. Second of all, consistent with the disappearance of MEPPC clinically observed during exercise, the triggered ventricular APs disappeared at higher pacing frequencies.

Therefore, the model confirms the mechanism by which the Na^+ channel alteration is responsible for the patients' phenotype.

Dilated cardiomyopathy is a secondary consequence of the mutation

SCN5A R222Q mutation was already detected in a few patients referred for familial or idiopathic DCM (41,42,40,13). However in all previously reported R222Q carriers, DCM was always associated with MEPPC-related ECG patterns. Mc Nair and collaborators identified 5 *SCN5A* mutations among 338 patients affected by DCM. Among them, 2 were carrier of the R222Q mutation and in both cases, patients were affected by frequent PVCs (>1000/h) and NSVT. Morales and collaborators investigated patients affected by peripartum cardiomyopathy and identified a family carrying the R222Q mutation, affected by DCM. In this family, 4 out of 6 carriers were also affected by ventricular or supra ventricular tachycardia (for one patient no information was available). In the families reported here, DCM was diagnosed in 6 individuals, and is very likely a consequence of the arrhythmia, and not directly linked to the mutation. Indeed, 13 patients affected by MEPPC, carriers of the R222Q *SCN5A* mutation, were not affected by DCM. Most importantly, the cardiomyopathy recovered at least partially under antiarrhythmic treatment after having reduced the number of PVCs. The low penetrance of the associated DCM phenotype in these

families suggests that the genetic background may play a role in the clinical evolution of the disease as now admitted even for monogenic cardiac arrhythmias (43). Several other *SCN5A* mutations associated with familial DCM-arrhythmia syndrome have also been described (R814W, D1275N, T220I and D1595H) (11,10,12). In these mutation carriers, predominant clinical findings were mainly sinus bradycardia, atrioventricular block, atrial fibrillation and/or atrial flutter, phenotypes quite different from the MEPPC syndrome. Therefore, our work does not rule out that DCM may be a primary consequence of other *SCN5A* mutations.

Hydroquinidine-based therapy

Because the treatment of the affected patients with hydroquinidine has been proven to be effective on PVCs, we investigated the effects of quinidine on the Na^+ currents and observed equivalent inhibition of WT and R222Q Nav1.5-mediated currents. Despite the fact that we did not consider the use-dependence of quinidine activity (44,45), the multicellular model recapitulates the effects of quinidine on PVCs suppression. Altogether, these results reinforce our hypothesis of MEPPC being the primary consequence of *SCN5A* R222Q mutation. Furthermore, it offers a potentially efficient therapy to limit the symptoms for *SCN5A* R222Q carriers. However it remains to be shown that the treatment may limit the risk of sudden death.

ACKNOWLEDGMENTS

We thank André Terzic, University of Minnesota, Minneapolis, Minn, for *ABCC9* sequencing and Béatrice Leray, *l'institut du thorax*, Nantes, France, for expert technical assistance with cell culture.

FIGURES LEGENDS

Figure 1

SCN5A mutation. (**A**) Pedigree and phenotype of the 5 families. Members affected with arrhythmia are indicated with a half-filled symbol. Members affected with arrhythmia and dilated cardiomyopathy (DCM) are indicated in black. Question marks indicate undetermined phenotype. Males and females are indicated by squares and circles, respectively. Probands are indicated by arrows. Diagonal lines indicate the deceased individuals. Individuals carrying the mutation are indicated (+). Individuals who tested negative for the mutation are indicated (-). An implantable cardioverter defibrillator (ICD) was implanted in 4 patients, 2 of them also had a cardiac resynchronization therapy defibrillator (CRTD) and 1, a DDD pace maker (DDD PM). Sudden death (SD) was reported in 5 individuals. (**B**) Mutation analysis of *SCN5A* revealed a heterozygous c.665G>A missense mutation in affected individual III.1 that results in a p.Arg222Gln (p.R222Q) amino-acid substitution. (**C**) Multiple alignment analysis shows conservation of the Arg222 (R222) amino-acid among species. (**D**) Structure of Nav1.5. The p.Arg222Gln mutation is located in the voltage-sensing S4 segment of domain I (DI).

Figure 2

Representative ECG tracings of the families. (**A**) Representative 12-lead surface ECG of family 1, 10-year old proband (individual III.1), showing a chaotic cardiac rhythm including normal sinus and junctional QRS complexes competing with various RBBB pattern complexes corresponding to PVCs. (**B**) Symptomatic NSVT recorded on the same patient as in (A), at 13 years old (RBBB pattern, QRS axis variation). QRS morphologies are changing from one beat to another. (**C**) Twelve-lead surface

ECG of patient III.1 of family 2 showing a chaotic cardiac rhythm with rare sinus beats and alternant junctional rhythms with ventricular bigeminisms. PVCs had LBBB pattern with slight variations in shape and axis.

Figure 3

Endocardial electroanatomic mapping of the left ventricle (**A**) Mapping of the left ventricle during sinus rhythm (patient II.4 family 1). Identification of the left specific conduction system. Pink and yellow tags present with a short sharp, high frequency and low amplitude potential preceding the ventricular electrograms (EGMs; arrows). Note that the area with yellow tags represent the His bundle region, and those with pink tags represent the left anterior and posterior fascicles. (**B-C**) Mapping of the left ventricle during ten different Purkinje-related ectopic contractions (same patient as in A). Identification of the different ectopic foci along the left specific conduction system. Pink and yellow tags as in A. Red tags indicate sites with single short sharp, high frequency and low amplitude potentials preceding the PVCs EGMs. Sites are labelled from 1 to 10 according to corresponding 12 lead PVC morphologies (recording at 100 mm/s). Ectopic sites during PVCs were identified along the Purkinje network (A) or the proximal extension of the left anterior and posterior fascicles. The arrows denote the Purkinje potentials. (**D**) Pace mapping from the same patient as in A. Right: 12-lead surface ECG (25mm/s) during PVC bigeminism. Left: pacing at the earliest local activation during PVCs (local presystolic potential), reproduced a very close match to the surface ECG (except for V1). Numbers are percentages of pacing concordance for each lead (from 45% at V1 to 99%, mean: 90%).

Figure 4

Experimental effects of R222Q mutation on Nav1.5 channel in COS-7 cells. (**A**) Relative peak conductance *vs.* membrane potential curves for Nav1.5 channels in COS-7 cells transfected with WT, R222Q Nav1.5 or both, in the presence of WT β1 subunit. Curves: Boltzmann fits to the data show the mutation-dependent activation shift. Inset: stimulation protocol and superimposed Na^+ current recordings during 20-ms depolarizations to various potentials from –80 to +0 mV (holding potential: –100 mV; 10-mV increment; frequency: 0.5 Hz). Scale bars: 2 ms, 1000 pA. Bold trace and arrow: Na^+ current at –50 mV. (**B**) Steady-state channel availability curves for Nav1.5 channels. Data are mean normalized peak current (I/I_{max}) measured at –20 mV *vs.* prepulse voltage. Curves: Boltzmann fits to the data. Inset: stimulation protocol and superimposed Na^+ current recordings at –20 mV after 500-ms polarization to various potentials from –110 to –50 mV (holding potential: –100 mV; 10-mV increment; frequency: 0.25 Hz) in COS-7 cells transfected as in A. Scale bar: 2 ms. Bold trace and arrow: Na^+ current at –80 mV. (**C**) Mean WT (n=13) and R222Q (n=14) tetrodotoxin-sensitive window currents (30 µM TTX) obtained with a depolarizing-voltage ramp (0.5 mV/ms, frequency: 0.5 Hz), normalized to the peak current at -20 mV (I_{peak}) recorded in the same cell (scale bar: 1% I_{peak}), and mean voltage at which the measured conductance was maximal (n=12 and 14, for WT and R222Q, respectively). ***: $p < 0.001$. (**D**) Effects of quinidine on WT and R222Q Nav1.5 currents. (*left*) Representative WT and R222Q Na^+ currents recordings during 20-ms depolarizations to –20 mV (holding potential: –100 mV; frequency: 0.5 Hz) in the absence (control) and presence of 30 µM quinidine (qui), and mean residual current ratio (I_{peak} qui/I_{peak} con) in each condition (bottom; n=12 and 10 for WT and R222Q, respectively). (*right*) Mean window tetrodotoxin-sensitive current density (30 µM TTX), in the absence and presence of 30 µM quinidine, of WT (thin line) and R222Q (bold

line) channels and mean residual current ratio (I_{max} qui/I_{max} con) measured when the conductance was maximal, in each condition (at –43 mV, n=6 and at –59 mV, n=7 for WT and R222Q, respectively). Scale bar: 2 pA/pF, same voltage protocol as in C.

Figure 5

Effects of the R222Q mutation on a ventricular cardiomyocyte action potential (AP) obtained in the Purkinje/ventricle model. (**A**) Dimensions of the calculation domain: Purkinje system, 5 x 17.5 mm; ventricle, 35 x 17.5 mm. Stimulation and recording sites are indicated. (**B**) and (**C**) Simulated AP in a distal part of the ventricle in WT (**a**) and heterozygous (**b**) conditions with stimulation of a Purkinje cell at cycle length of 1 s (**B**) and 0.5 s (**C**); and in the presence of quinidine (**Bb**; i.e. remaining 75% heterozygous INa, 45% WT Ito and 45% WT IKr; red) at 1 Hz.

TABLES

REFERENCES

1 Kaufman ES. Mechanisms and clinical management of inherited channelopathies: long QT syndrome, Brugada syndrome, catecholaminergic polymorphic ventricular tachycardia, and short QT syndrome. Heart Rhythm 2009;6:S51-S55.

2 Mohler PJ, Schott JJ, Gramolini AO et al. Ankyrin-B mutation causes type 4 long-QT cardiac arrhythmia and sudden cardiac death. Nature 2003;421:634-9.

3 Watanabe H, Koopmann TT, Le Scouarnec S et al. Sodium channel beta1 subunit mutations associated with Brugada syndrome and cardiac conduction disease in humans. J Clin Invest 2008;118:2260-8.

4 Hedley PL, Jorgensen P, Schlamowitz S et al. The genetic basis of long QT and short QT syndromes: a mutation update. Hum Mutat 2009;30:1486-511.

5 Zimmer T, Surber R. SCN5A channelopathies - an update on mutations and mechanisms. Prog Biophys Mol Biol 2008;98:120-36.

6 Tfelt-Hansen J, Winkel BG, Grunnet M, Jespersen T. Inherited cardiac diseases caused by mutations in the Nav1.5 sodium channel. J Cardiovasc Electrophysiol 2010;21:107-15.

7 Rook MB, Bezzina AC, Groenewegen WA et al. Human SCN5A gene mutations alter cardiac sodium channel kinetics and are associated with the Brugada syndrome. Cardiovasc Res 1999;44:507-17.

8 Schott JJ, Alshinawi C, Kyndt F et al. Cardiac conduction defects associate with mutations in SCN5A. Nat Genet 1999;23:20-1.

9 Probst V, Kyndt F, Potet F et al. Haploinsufficiency in combination with aging causes SCN5A-linked hereditary Lenegre disease. J Am Coll Cardiol 2003;41:643-52.

10 Olson TM, Michels VV, Ballew JD et al. Sodium channel mutations and susceptibility to heart failure and atrial fibrillation. JAMA 2005;293:447-54.

11 McNair WP, Ku L, Taylor MR et al. SCN5A mutation associated with dilated cardiomyopathy, conduction disorder, and arrhythmia. Circulation 2004;110:2163-7.

12 Nguyen TP, Wang DW, Rhodes TH, George AL, Jr. Divergent biophysical defects caused by mutant sodium channels in dilated cardiomyopathy with arrhythmia. Circ Res 2008;102:364-71.

13 McNair WP, Sinagra G, Taylor MR et al. SCN5A Mutations Associate With Arrhythmic Dilated Cardiomyopathy and Commonly Localize to the Voltage-Sensing Mechanism. J Am Coll Cardiol 2011;57:2160-8.

14 Remme CA, Wilde AA, Bezzina CR. Cardiac sodium channel overlap syndromes: different faces of SCN5A mutations. Trends Cardiovasc Med 2008;18:78-87.

15 Wolf CM, Wang L, Alcalai R et al. Lamin A/C haploinsufficiency causes dilated cardiomyopathy and apoptosis-triggered cardiac conduction system disease. J Mol Cell Cardiol 2008;44:293-303.

16 Bienengraeber M, Olson TM, Selivanov VA et al. ABCC9 mutations identified in human dilated cardiomyopathy disrupt catalytic KATP channel gating. Nat Genet 2004;36:382-7.

17 Genin E, Tullio-Pelet A, Begeot F, Lyonnet S, Abel L. Estimating the age of rare disease mutations: the example of Triple-A syndrome. J Med Genet 2004;41:445-9.

18 Allouis M, Le Bouffant F, Wilders R et al. 14-3-3 is a regulator of the cardiac voltage-gated sodium channel Nav1.5. Circ Res 2006;98:1538-46.

19 DiFrancesco D, Noble D. A model of cardiac electrical activity incorporating ionic pumps and concentration changes. Philos Trans R Soc Lond B Biol Sci 1985;307:353-98.

20 Iyer V, Mazhari R, Winslow RL. A computational model of the human left-ventricular epicardial myocyte. Biophys J 2004;87:1507-25.

21 Keener J, Sneyd J. Mathematical Physiology , 2nd edition. Springer, 2001.

22 Aslanidi OV, Stewart P, Boyett MR, Zhang H. Optimal velocity and safety of discontinuous conduction through the heterogeneous Purkinje-ventricular junction. Biophys J 2009;97:20-39.

23 Kampmann C, Wiethoff CM, Wenzel A et al. Normal values of M mode echocardiographic measurements of more than 2000 healthy infants and children in central Europe. Heart 2000;83:667-72.

24 Nogami A, Naito S, Tada H et al. Demonstration of diastolic and presystolic Purkinje potentials as critical potentials in a macroreentry circuit of verapamil-sensitive idiopathic left ventricular tachycardia. J Am Coll Cardiol 2000;36:811-23.

25 Reithmann C, Hahnefeld A, Ulbrich M, Matis T, Steinbeck G. Different forms of ventricular tachycardia involving the left anterior fascicle in nonischemic cardiomyopathy: critical sites of the reentrant circuit in low-voltage areas. J Cardiovasc Electrophysiol 2009;20:841-9.

26 Tanner H, Hindricks G, Volkmer M et al. Catheter ablation of recurrent scar-related ventricular tachycardia using electroanatomical mapping and irrigated ablation technology: results of the prospective multicenter Euro-VT-study. J Cardiovasc Electrophysiol 2010;21:47-53.

29

27 Imaizumi Y, Giles WR. Quinidine-induced inhibition of transient outward current in cardiac muscle. Am J Physiol 1987;253:H704-H708.

28 Wang Z, Fermini B, Nattel S. Effects of flecainide, quinidine, and 4-aminopyridine on transient outward and ultrarapid delayed rectifier currents in human atrial myocytes. J Pharmacol Exp Ther 1995;272:184-96

29 Roden DM, Bennett PB, Snyders DJ, Balser JR, Hondeghem LM. Quinidine delays IK activation in guinea pig ventricular myocytes. Circ Res 1988;62:1055-8.

30 Sanchez-Chapula JA, Ferrer T, Navarro-Polanco RA, Sanguinetti MC. Voltage-dependent profile of human ether-a-go-go-related gene channel block is influenced by a single residue in the S6 transmembrane domain. Mol Pharmacol 2003;63:1051-8.

31 Salata JJ, Wasserstrom JA. Effects of quinidine on action potentials and ionic currents in isolated canine ventricular myocytes. Circ Res 1988;62:324-37.

32 Iost N, Virag L, Varro A, Papp JG. Comparison of the effect of class IA antiarrhythmic drugs on transmembrane potassium currents in rabbit ventricular myocytes. J Cardiovasc Pharmacol Ther 2003;8:31-41.

33 Wu L, Guo D, Li H et al. Role of late sodium current in modulating the proarrhythmic and antiarrhythmic effects of quinidine. Heart Rhythm 2008;5:1726-34.

34 Lopera G, Stevenson WG, Soejima K et al. Identification and ablation of three types of ventricular tachycardia involving the His-Purkinje system in patients with heart disease. J Cardiovasc Electrophysiol 2004;15:52-8.

35 Rodriguez LM, Smeets JL, Timmermans C, Trappe HJ, Wellens HJ. Radiofrequency catheter ablation of idiopathic ventricular tachycardia originating

in the anterior fascicle of the left bundle branch. J Cardiovasc Electrophysiol 1996;7:1211-6.

36 Doppalapudi H, Yamada T, McElderry HT, Plumb VJ, Epstein AE, Kay GN. Ventricular tachycardia originating from the posterior papillary muscle in the left ventricle: a distinct clinical syndrome. Circ Arrhythm Electrophysiol 2008;1:23-9.

37 Kapplinger JD, Tester DJ, Alders M et al. An international compendium of mutations in the SCN5A-encoded cardiac sodium channel in patients referred for Brugada syndrome genetic testing. Heart Rhythm 2010;7:33-46.

38 Kapplinger JD, Tester DJ, Salisbury BA et al. Spectrum and prevalence of mutations from the first 2,500 consecutive unrelated patients referred for the FAMILION long QT syndrome genetic test. Heart Rhythm 2009;6:1297-303.

39 Makita N. Phenotypic overlap of cardiac sodium channelopathies: individual-specific or mutation-specific? Circ J 2009;73:810-7.

40 Cheng J, Morales A, Siegfried JD et al. SCN5A rare variants in familial dilated cardiomyopathy decrease peak sodium current depending on the common polymorphism H558R and common splice variant Q1077del. Clin Transl Sci 2010;3:287-94.

41 Hershberger RE, Parks SB, Kushner JD et al. Coding sequence mutations identified in MYH7, TNNT2, SCN5A, CSRP3, LBD3, and TCAP from 313 patients with familial or idiopathic dilated cardiomyopathy. Clin Transl Sci 2008;1:21-6.

42 Morales A, Painter T, Li R et al. Rare variant mutations in pregnancy-associated or peripartum cardiomyopathy. Circulation 2010;121:2176-82.

43 Roden DM. Human genomics and its impact on arrhythmias. Trends Cardiovasc Med. 2004;14:112-6.

44 Snyders DJ, Hondeghem LM. Effects of quinidine on the sodium current of guinea pig ventricular myocytes. Evidence for a drug-associated rested state with altered kinetics. Circ Res 1990;66:565-79.

45 Yang T, Roden DM. Extracellular potassium modulation of drug block of IKr. Implications for torsade de pointes and reverse use-dependence. Circulation 1996;93:407-11.

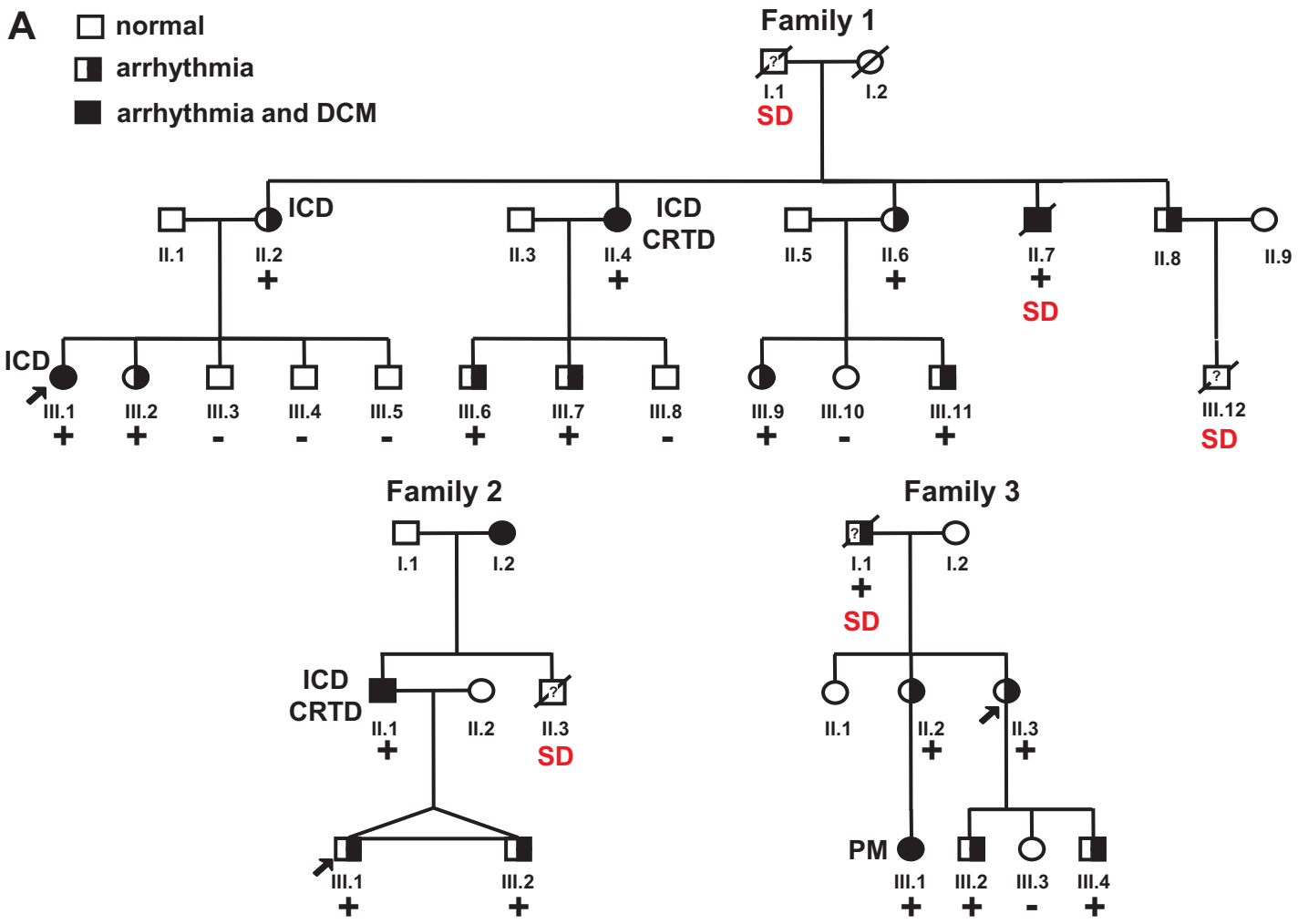
A
normal
arrhythmia
arrhythmia and DCM
Family 1
I.1
SD
I.2
ICD
II.1
II.2
+
II.3
II.4
+
ICD
CRTD
II.5
II.6
+
II.7
+
SD
II.8
II.9
ICD
III.1
+
III.2
+
III.3
-
III.4
-
III.5
-
III.6
+
III.7
+
III.8
-
III.9
+
III.10
-
III.11
+
III.12
SD
Family 2
I.1
I.2
ICD
CRTD
II.1
+
II.2
II.3
SD
III.1
+
III.2
+
Family 3
I.1
+
SD
I.2
II.1
II.2
+
II.3
+
PM
III.1
+
III.2
+
III.3
-
III.4
+

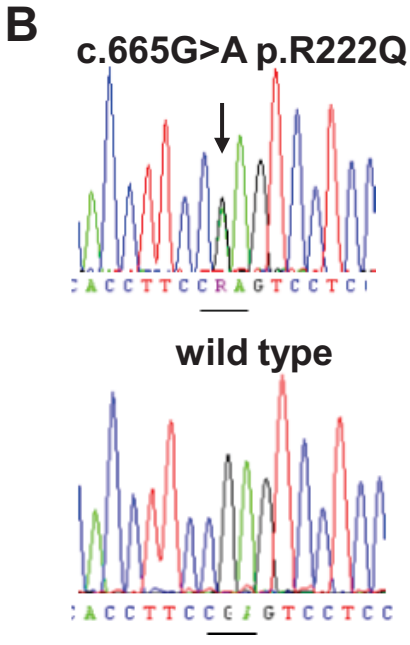
B
c.665G>A p.R222Q
wild type

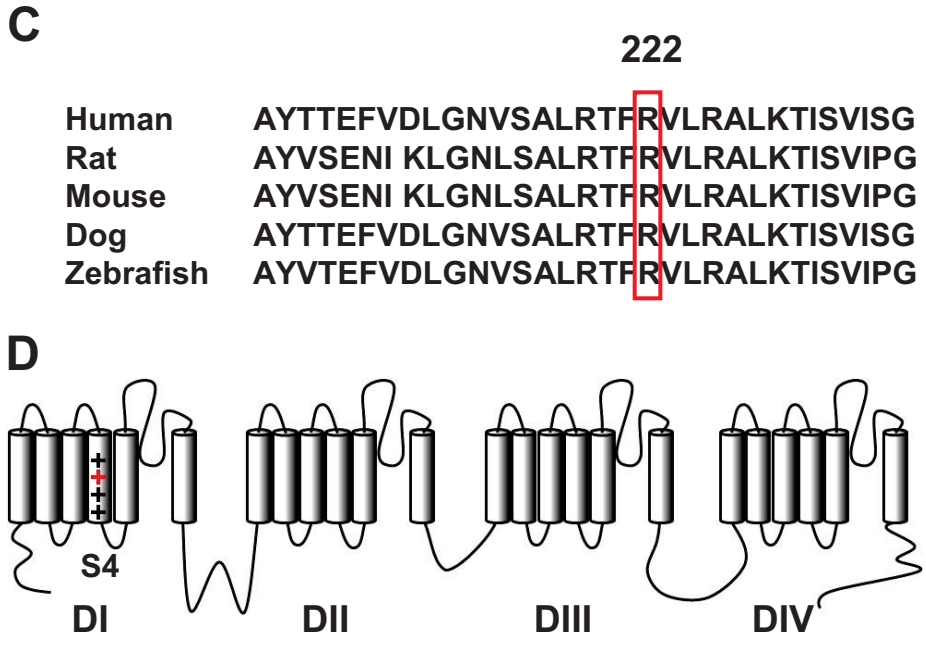
C
222
Human AYTTEFVDLGNVSALRTFRVLRALKTISVISG
Rat AYVSENI KLGNLSALRTFRVLRALKTISVIPG
Mouse AYVSENI KLGNLSALRTFRVLRALKTISVIPG
Dog AYTTEFVDLGNVSALRTFRVLRALKTISVISG
Zebrafish AYVTEFVDLGNVSALRTFRVLRALKTISVIPG
D
S4
DI
DII
DIII
DIV

figure 1

A **patient III.1 family 1 at 10 years old**

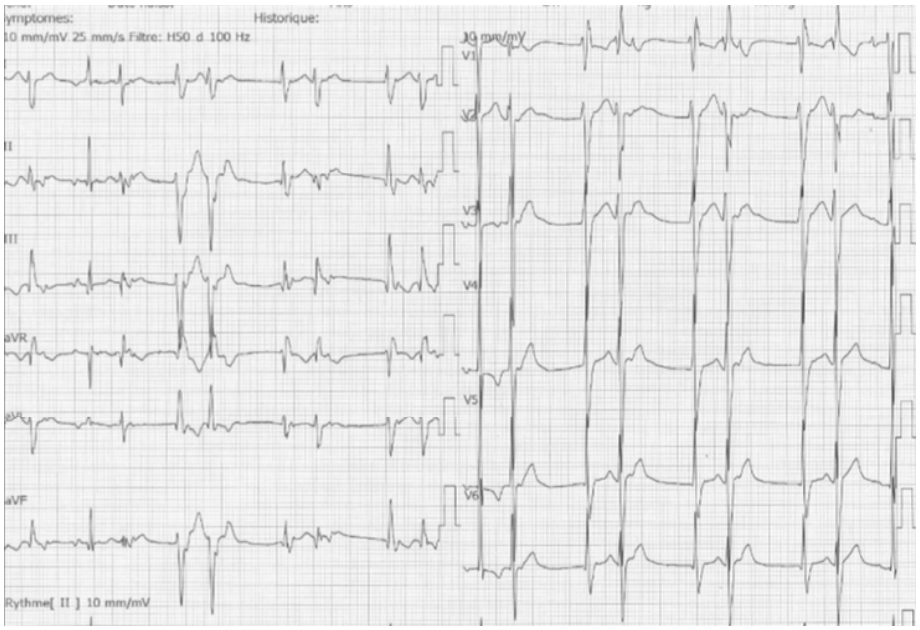

B **patient III.1 family 1 at 13 years old**

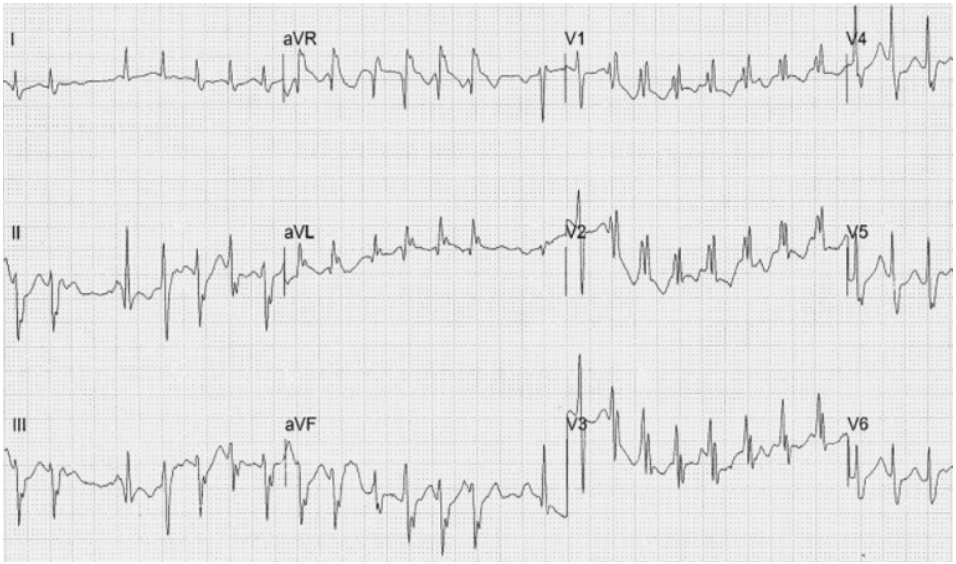

C **patient III.1 family 2**

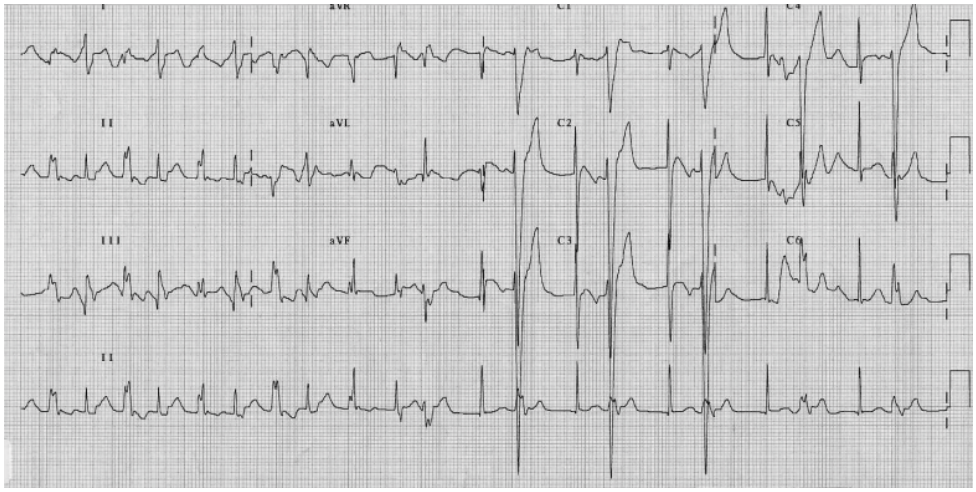

figure 2

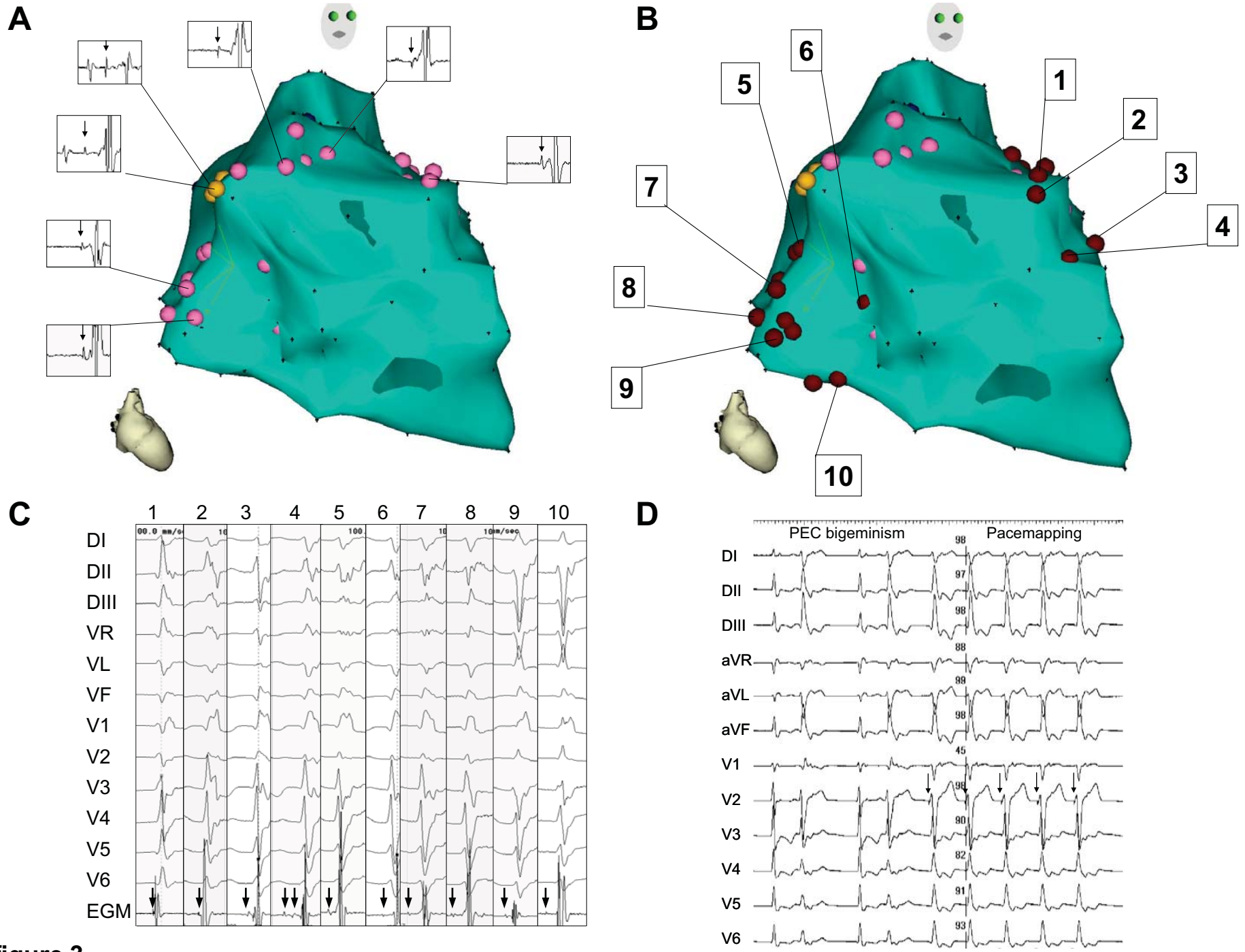
A
B
1
2
3
4
5
6
7
8
9
10
C
1 2 3 4 5 6 7 8 9 10
DI
DII
DIII
VR
VL
VF
V1
V2
V3
V4
V5
V6
EGM
D
PEC bigeminism
Pacemapping
DI
DII
DIII
aVR
aVL
aVF
V1
V2
V3
V4
V5
V6

figure 3

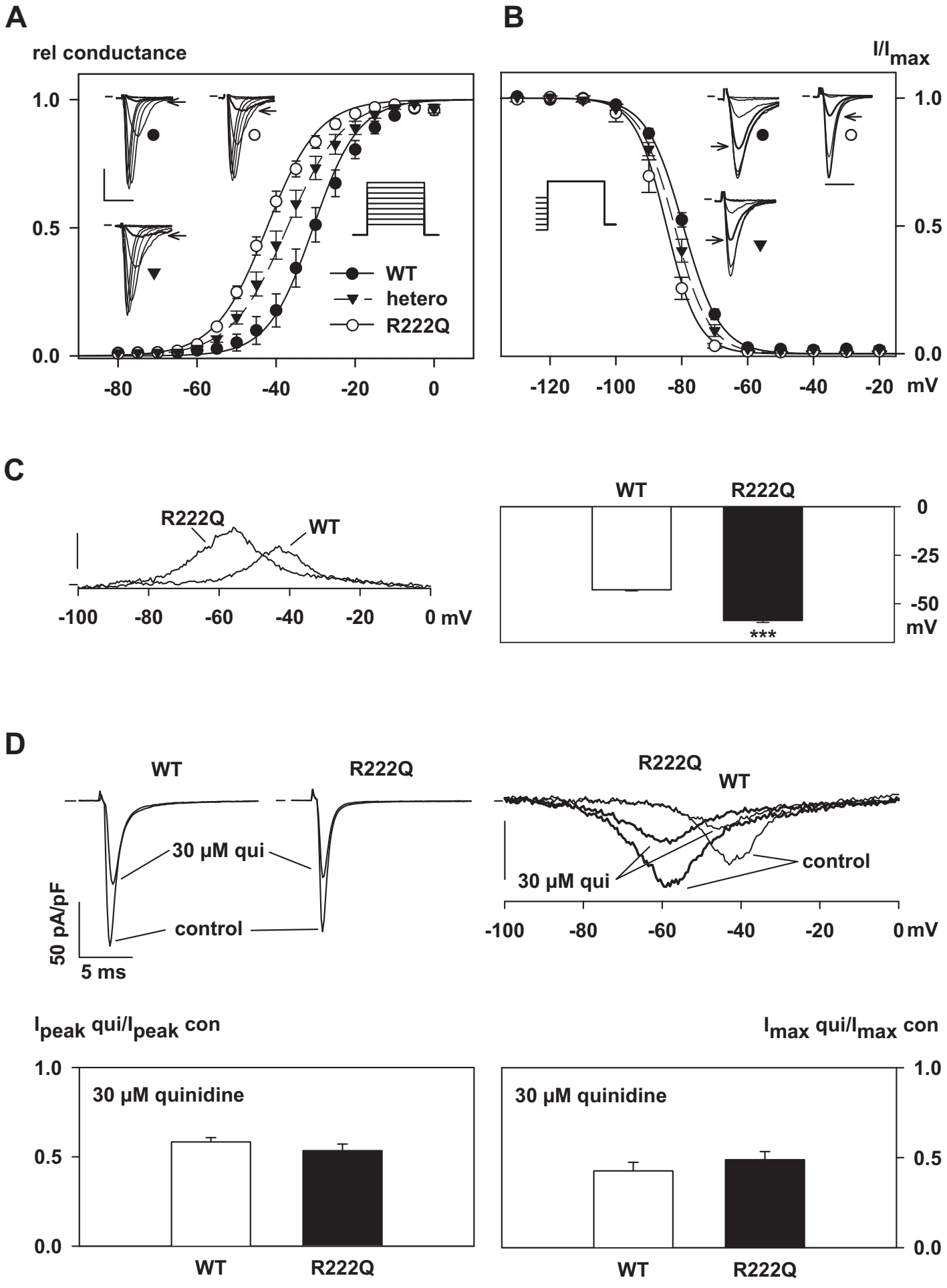
A
rel conductance
1.0
0.5
0.0
-80
-60
-40
-20
0
WT
hetero
R222Q
B
I/I max
1.0
0.5
0.0
-120
-100
-80
-60
-40
-20
mV
C
R222Q
WT
-100
-80
-60
-40
-20
0 mV
WT
R222Q
0
-25
-50
mV
***
D
WT
R222Q
30 µM qui
control
50 pA/pF
5 ms
R222Q
WT
30 µM qui
control
-100
-80
-60
-40
-20
0 mV
I peak qui/I peak con
30 µM quinidine
1.0
0.5
0.0
WT
R222Q
I max qui/I max con
30 µM quinidine
1.0
0.5
0.0
WT
R222Q

figure 4

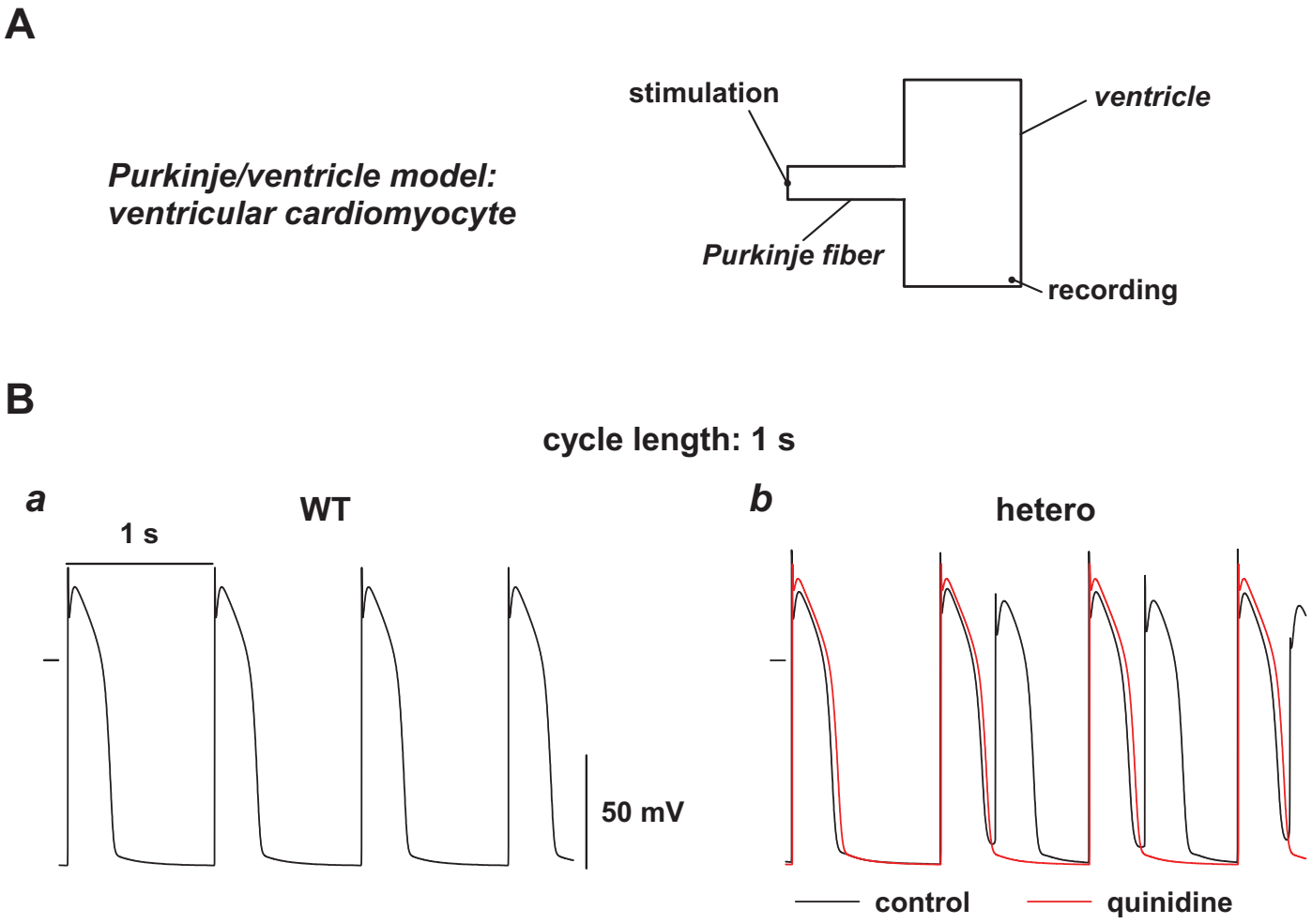
A
Purkinje/ventricle model:
ventricular cardiomyocyte
stimulation
ventricle
Purkinje fiber
recording
B
cycle length: 1 s
a
WT
1 s
50 mV
b
hetero
control
quinidine
C
cycle length: 0.5 s
a
WT
0.5 s
50 mV
b
hetero

figure 5